Check for updates

How to cite: *Angew. Chem. Int. Ed.* **2021**, *60*, 3906–3911
International Edition: doi.org/10.1002/anie.202014696
German Edition: doi.org/10.1002/ange.202014696

Perovskites | Hot Paper

Mixed Group 14–15 Metalates as Model Compounds for Doped Lead Halide Perovskites

Natalie Dehnhardt, Jan-Niclas Luy, Philip Klement, Luca Schipplick, Sangam Chatterjee, Ralf Tonner, and Johanna Heine**

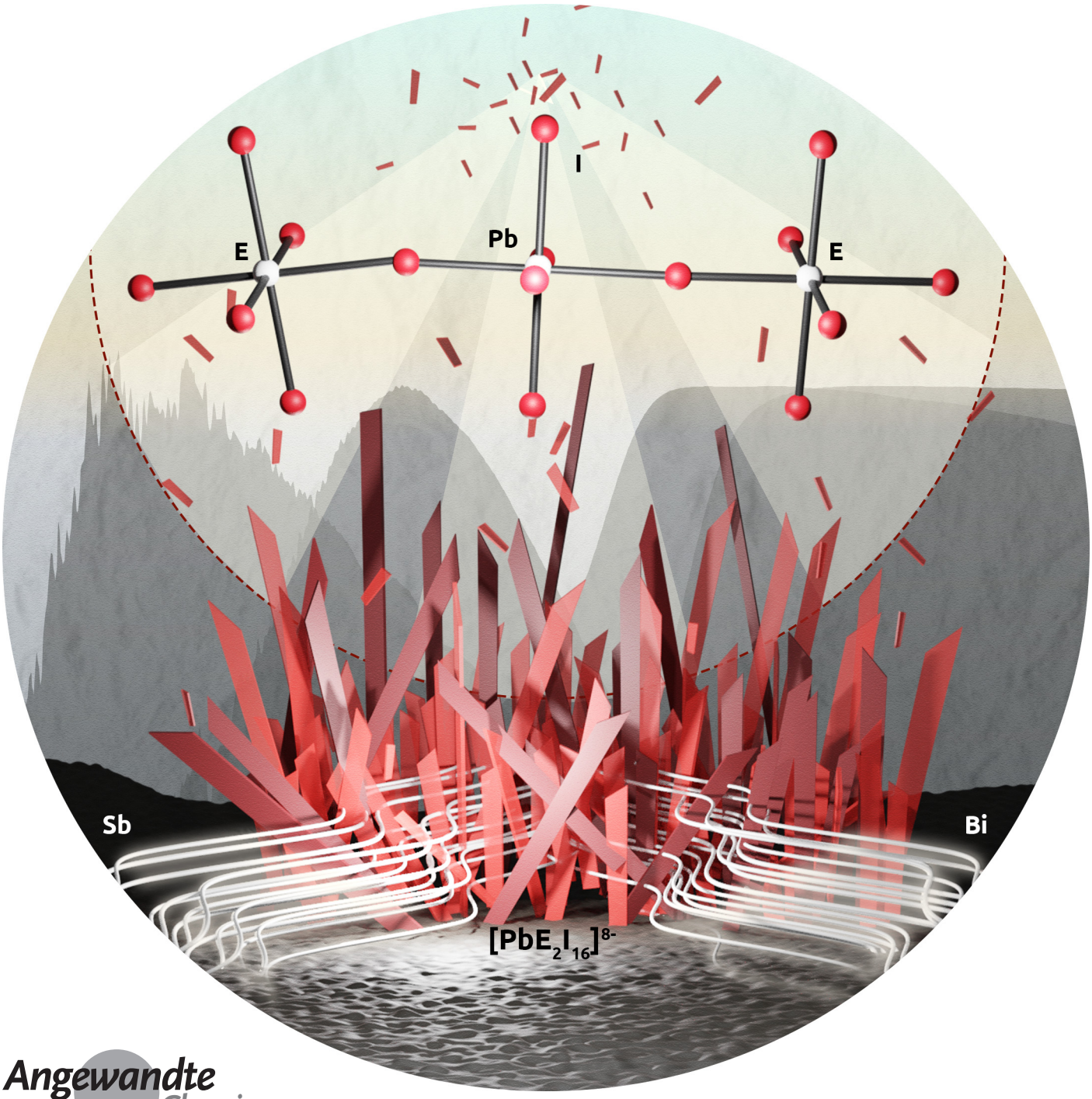

 © 2020 The Authors. Angewandte Chemie International Edition published by Wiley-VCH GmbH

Abstract: *Doping and alloying are valuable tools for modifying and enhancing the properties and performance of lead halide perovskites. However, the effects of heterovalent doping with Sb^{3+} and Bi^{3+} cations are still a matter of current investigation. Due to the different charge of the dopants compared to the constituting Pb^{2+} ions, a simultaneous creation of defects is unavoidable and the influence of these defects and the actual metal substitution become entangled. Herein, we present the first 14–15 iodido metalates, $(BED)_4PbE_2I_{16}$ (BED = N-benzylethylenediammonium; E = Sb (**1**), Bi (**2**)), which are model compounds for doped lead iodide perovskites and display surprisingly low band gaps of 2.01 (**1**) and 1.88 eV (**2**). Quantum chemical investigations show that this stems from a good electronic match between the PbI_6 and EI_6 units of the compounds. Our results provide a model system for doped perovskites, but also represent the first examples of a promising new class of metal halide materials.*

Hybrid halide perovskites like $(CH_3NH_3)PbI_3$ are of great current interest due to their excellent semiconductor properties.[1–3] Applications include photovoltaics, solid state lighting, lasers, and photocatalysts.[4–7] The physics behind the properties of hybrid halide perovskites are a subject of ongoing investigations[8] and many researchers have modified and broadened these properties through approaches like dimensional reduction or the preparation of nanoparticles.[9,10] Two additional approaches are doping and alloying.[11–13] All three sites of AMX_3 perovskites (A = organic or inorganic cation; M = Sn or Pb; X = Cl, Br, I) can be modified this way, with A and X site doping and alloying being used to produce solar cells with record performance.[14,15] This way it is also possible to tune the materials' band gap, increase their stability and introduce new photoluminescence properties.[16–18]

One area of ongoing research and scientific debate are lead halide perovskites doped with antimony or bismuth, $APbX_3$:E (E = Sb, Bi). Bakr and co-workers were the first to report an example of this class of materials, $(CH_3NH_3)PbBr_3$:Bi, with Bi contents of up to 0.3%. They found that even at small Bi concentrations, an enhancement of electrical conductivity and a change in the sign of majority charge carriers from positive to negative could be observed. They also observed a darkening of the crystal color and proposed that this is due to band gap narrowing.[19] However, subsequent investigations showed that the color change is due to the introduction of defects.[20–22] The effect of bismuth doping on the photovoltaic performance of lead iodide perovskites is a point of ongoing research: Troshin and Tress found that Bi doping is highly detrimental to the power conversion efficiency of $(CH_3NH_3)PbI_3$ solar cells.[23,24] In contrast, Zhang found that Bi doping increases the moisture tolerance and power conversion efficiency in $(FA)PbI_3$-based devices (FA = formamidinium).[25]

Antimony-doped lead halide perovskites have also been synthesized, showing a better stability and photovoltaic performance than their undoped counterparts.[26–28] It is often unclear if changes in properties are the direct result of doping, or if a phase segregation during synthesis or under bias is occurring, as recently shown for antimony-doped materials.[29] A separation into a material with a bismuth- or antimony-rich protective layer may be beneficial, as intentional preparations of such materials have shown.[30–32]

Quantum chemical studies have been performed to elucidate the effects of $APbX_3$:E doping, but it is not clear how the charge mismatch of the Bi^{3+} ion is compensated by additional defects under different synthesis conditions.[33–35] Despite these remaining questions, it has been demonstrated that Sb and Bi doping can introduce useful new properties into lead halide perovskites, such as photoluminescence in the near infrared,[36,37] improved photoluminescence quantum yield in blue-emitting $CsPbBr_3$ nanocrystals,[38] improved thermoelectric properties,[39] and that co-doping approaches can help to avoid defect formation caused by the charge mismatch between Pb^{2+} and Sb^{3+} or Bi^{3+}.[40] Overall, it is clear that model compounds featuring the same coordination environment and connectivity as is assumed to be present in $APbX_3$:E are urgently needed to elucidate and disentangle the effects observed in these materials.

Herein, we present the organic–inorganic 14–15 halogenido metalates $(BED)_4PbE_2I_{16}$ (BED = *N*-benzylethylenediammonium; E = Sb (**1**), Bi (**2**)). Inspired by recent work on cuprates using BED,[41] we aimed to produce layered group 14–15 perovskites, similar to examples introduced by Solis-Ibarra.[42–44] Somewhat puzzling, mixed 14–15 halogenido metalates have been restricted to the stabilization of polycationic clusters, as shown by Ruck.[45–48] Ma recently reported $(bmpy)_9[SbCl_5]_2[Pb_3Cl_{11}]$ (bmpy = 1-butyl-1-methylpyrrolidinium), a compound featuring both antimonate and plumbate anions, but no direct connection E^{14}-X-E^{15}.[49] This highlights a potential difficulty in the synthesis of group 14–15 halogen-

[*] Dr. N. Dehnhardt, L. Schipplick, Dr. J. Heine
Department of Chemistry and Material Sciences Center
Philipps-Universität Marburg
Hans-Meerwein-Strasse, 35043 Marburg (Germany)
E-mail: johanna.heine@chemie.uni-marburg.de
J.-N. Luy, Prof. Dr. R. Tonner
Faculty of Chemistry and Pharmacy
University of Regensburg
Universitätsstrasse 31, 93053 Regensburg (Germany)
P. Klement, Prof. Dr. S. Chatterjee
Institute of Experimental Physics I and Center for Materials Research (ZfM)
Justus Liebig University Giessen
Heinrich-Buff-Ring 16, 35392 Giessen (Germany)
Prof. Dr. R. Tonner
Current address: Wilhelm-Ostwald-Institut für Physikalische und Theoretische Chemie
Universität Leipzig
Linnéstrasse 2, 04103 Leipzig (Germany)
E-mail: ralf.tonner@uni-leipzig.de
Supporting information and the ORCID identification number(s) for the author(s) of this article can be found under: https://doi.org/10.1002/anie.202014696.

© 2020 The Authors. Angewandte Chemie International Edition published by Wiley-VCH GmbH. This is an open access article under the terms of the Creative Commons Attribution Non-Commercial NoDerivs License, which permits use and distribution in any medium, provided the original work is properly cited, the use is non-commercial and no modifications or adaptations are made.

15213773, 2021, 8, Downloaded from https://onlinelibrary.wiley.com/doi/10.1002/anie.202014696 by Universitaet Regensburg, Wiley Online Library on [18/03/2024]. See the Terms and Conditions (https://onlinelibrary.wiley.com/terms-and-conditions) on Wiley Online Library for rules of use; OA articles are governed by the applicable Creative Commons License

ido metalates, as the formation of separate E^{14}–X and E^{15}–X anions can be an issue.

We found that the anions in **1** and **2** are not layered but molecular, composed of three corner-sharing octahedra, with the PbI_6 unit in the middle. They represent the first model compounds for $APbX_3$:E and allow us to investigate the Pb–E interaction in detail through the compounds' optical properties and quantum chemical studies, which reveal a strong interaction leading to a comparatively low band gap for compounds containing molecular metalate anions. This demonstrates that 14–15 halogenido metalates are promising new materials that may be able to enhance the useful properties of their parent metalates.

1 and **2** can be prepared by combining PbO, Sb_2O_3, or Bi_2O_3 and N-benzylethylenediamine in two molar hydriodic acid solution (Figure 1), a route reported earlier for simple plumbates and pentelates.[50,51]

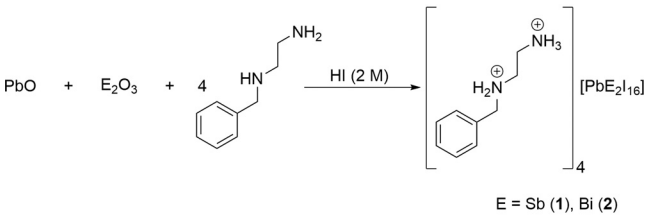

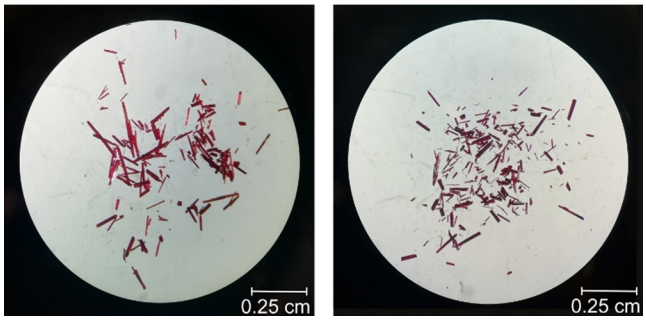

Figure 1. Reaction Scheme (top) and photographs of crystals of **1** and **2** (bottom left and bottom right).

The two compounds crystallize as intergrown red (**1**) or dark red (**2**) planks (Figure 1). Both compounds are isomorphous, crystallizing in the monoclinic space group $P2_1/n$ (No. 14). An excerpt of the crystal structure of **1** is shown in Figure 2a. Bond lengths in the trinuclear $[PbE_2I_{16}]^{8-}$ anions are given in Figure 2b. They are in similar ranges as found for binary pentelates with $[EI_6]^{3-}$ anions, such as $(Pip)_3[SbI_6]_2{\cdot}5H_2O$ (Pip = piperazine-1,4-diium; Sb–I bond lengths: 2.85–3.26 Å) and $(DMA)_3BiI_6$ (DMA = dimethylammonium; Bi–I-bond lengths: 3.03–3.09 Å).[52,53] Pb–I distances are similar to those found in $(CH_3NH_3)PbI_3$ (Pb–I bond lengths: 3.175–3.180 Å). This highlights that **1** and **2** are good models for $APbX_3$:E doping.[54] The relative arrangement of the octahedra is fairly regular, exhibiting slight tilting along the E-I-Pb connection, with an angle of 164° in **1** and 162° in **2**. Pb and Bi cannot be differentiated during crystal structure refinement, but the isomorphous nature of **1** and **2** and the results of elemental analysis strongly suggest that the arrangement of E and Pb atoms is the same in both compounds.

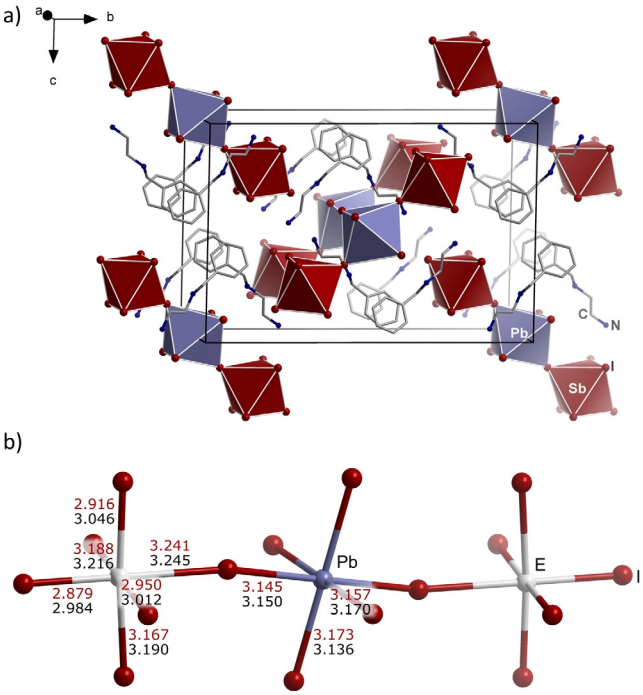

Figure 2. a) Excerpt of the crystal structure of **1**.[71] b) Trinuclear anion $[PbE_2I_{16}]^{8-}$ with bond lengths in angstrom for **1** (red) and **2** (black).

Trinuclear halogenido metalates with corner-sharing octahedra are rare, but have been reported before.[55–57] The organic cations separate the individual anions in such a way that no short intermolecular iodine–iodine contacts are observed in **1** and **2**.

We analyzed the thermal stability and found that **1** and **2** start to decompose at 260 and 266 °C (Figures S5, S6), similar to 2D perovskites like $(C_4H_9NH_3)_2PbI_4$, which decomposes at 285 °C.[58] Furthermore, both compounds are long-time stable in air, showing no signs of decomposition after months of storage.

The optical properties of **1** and **2** shed light on the fundamental electronic processes in both materials, and allow for the identification of the structure–property relationship. Both **1** and **2** exhibit absorption in the red part of the visible spectrum (Figure 3) as implied from their visual appearance (Figure 1). The band gap energies (E_g) determined from Tauc plots at cryogenic temperatures (3.5 K) are 2.08 (**1**) and 1.94 eV (**2**) (Figure S9). At 300 K, values of 2.01 (**1**) and 1.88 eV (**2**) were observed (Figure S10). This is considerably lower than the band gap of binary metalates with anions of the same dimensionality. Typical iodido plumbates with molecular anions have band gaps in the range of 2.9–3.2 eV.[59] Iodido antimonates and bismuthates with mononuclear anions display band gaps of 2.2 and 2.1 eV, respectively.[60] This suggests a significant electronic interaction between the EI_6 and PbI_6 units in **1** and **2**, which we elucidate with quantum chemical methods (see below). The incorporation of Bi reduces the band gap by 0.14 eV. Furthermore, it introduces a considerable amount of absorption below the band gap energy E_g known as Urbach tail. This can have several points of origin, e.g., lattice distortion[61] or the formation of

 © 2020 The Authors. Angewandte Chemie International Edition published by Wiley-VCH GmbH

15213773, 2021, 8, Downloaded from https://onlinelibrary.wiley.com/doi/10.1002/anie.202014696 by Universitaet Regensburg, Wiley Online Library on [18/03/2024]. See the Terms and Conditions (https://onlinelibrary.wiley.com/terms-and-conditions) on Wiley Online Library for rules of use; OA articles are governed by the applicable Creative Commons License

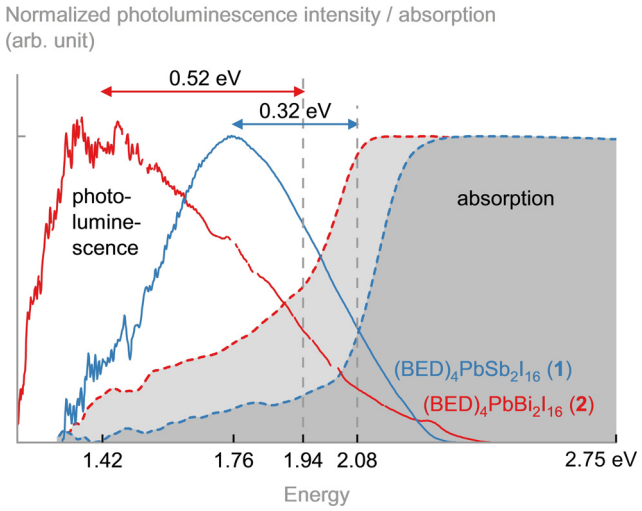

Figure 3. Optical properties of $(BED)_4PbSb_2I_{16}$ (**1**) and $(BED)_4PbBi_2I_{16}$ (**2**) at 3.5 K. Both exhibit absorption in the red part of the visible spectrum and a considerably Stokes-shifted photoluminescence feature at the border to the near-infrared range. The excitation energy was 3.06 eV (405 nm).

defect states in the band gap. In our case, this is also evidenced in the single crystal structure of **2**, which features more strongly disordered organic cations than found in **1**.

We performed photoluminescence spectroscopy to determine the emission properties of **1** and **2**, and relate them to the incorporation of Sb and Bi. The photoluminescence of **1** and **2** shows broad emission bands centered in the red and near-infrared part of the electromagnetic spectrum (Figure 3). The photoluminescence is centered at 1.76 (**1**) and 1.42 eV (**2**), with full width at half maximum (FWHM) of 0.5 (**1**) and 0.6 eV (**2**). Both are considerably red-shifted from the band gap energy E_g by 0.32 (**1**) and 0.52 eV (**2**), respectively. Such spectrally broad photoluminescence emissions features and large Stokes shifts are generally interpreted as an indication of strong electron–phonon coupling in these materials.[62,63] The strong electron–phonon coupling and our observation of a very soft structure (cf. description in the SI) set up the conditions for the formation of self-trapped excitons. The larger Stokes shift upon Bi incorporation can be explained in this context as Bi inducing a larger lattice deformation, which is consistent with the appearance of an Urbach tail in the absorption.

We performed density functional theory (DFT) computations to study the origin of the small band gap. The structure was optimized with GGA-type functional PBE[64] including dispersion interaction method DFT-D3[65,66] with periodic boundary conditions (see SI for details). The resulting cell volume was reduced by about 8%. This rather large difference is probably due to the flexible nature of the crystal. Band gaps (Table 1) were then derived with meta-GGA TB09[67] including spin orbit coupling (SOC) effects. This approach was used successfully in the past for similar systems.[68] While PBE (without SOC) already gives reasonably accurate band gaps for **1** and **2**, the trend is reproduced wrongly. This is corrected by the more reliable TB09 functional which gives values in very good agreement with experiment and correctly

Table 1: Computed band gaps in comparison to experimental data.

E_g [eV]	**1**	**2**
Experimental (300 K)	2.01	1.88
PBE	1.78	1.88
TB09-SOC	1.99	1.78

predicts **1** to have a larger band gap. This agrees with previous findings on optical properties of similar perovskites.[69]

The partial density of states (pDOS, Figure 4) around the Fermi energy gives a more thorough understanding of the band gap's nature. The valence band (VB) of **1** is primarily formed by an antibonding interaction of lone pairs at iodine with the Pb 6s orbital (left inset in Figure 4 and Figure S12 in the SI). Contributions by Sb or the organic cations are minor. The conduction band (CB) on the other hand has a σ* character along the I-Sb-Pb chain (right inset in Figure 4 and Figure S13 in the SI). For isostructural compound **2** a very similar electronic structure of the VB and CB is found resulting in a comparable band gap (see Figures S11, S14, and S15).

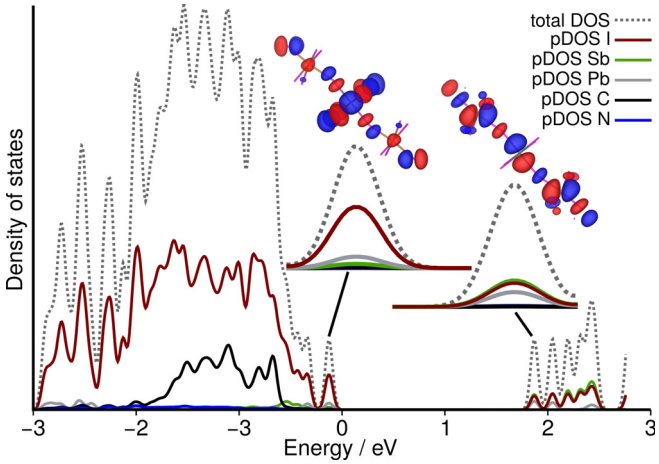

Figure 4. Total and partial density of states (pDOS) of **1**. Insets show magnification of the valence band and conduction band regions together with their real-space representation.

Our results show that both antimony and bismuth are capable of providing significant electronic modifications in lead halide perovskite materials beyond the creation of specific defects. The strong electronic interaction of the PbI_6 and EI_6 units suggests that when further examples of 14–15 iodido metalates are prepared, their structural and electronic dimensionality will coincide.[70] This raises the prospect that in these materials the beneficial properties of the constituting metalates can be combined and enhanced, for example into layered metalates with low band gaps, good charge carrier mobility, and excellent stability.

In summary, we have prepared the first 14–15 iodido metalates $(BED)_4PbE_2I_{16}$ (E = Sb (**1**), Bi (**2**)). The compounds feature trinuclear anions that represent precise cutouts of Sb- or Bi-doped perovskites $APbI_3$:E. **1** and **2** are long-term stable in air and display surprisingly low band gaps of

 © 2020 The Authors. Angewandte Chemie International Edition published by Wiley-VCH GmbH

15213773, 2021, 8, Downloaded from https://onlinelibrary.wiley.com/doi/10.1002/anie.202014696 by Universitaet Regensburg, Wiley Online Library on [18/03/2024]. See the Terms and Conditions (https://onlinelibrary.wiley.com/terms-and-conditions) on Wiley Online Library for rules of use; OA articles are governed by the applicable Creative Commons License

2.01 and 1.88 eV. Quantum chemical investigations show that these can be traced to a strong electronic interaction between the PbI_6 and EI_6 units, with a valence band maximum featuring major contributions of Pb and I, while the conduction band minimum shows contributions from Pb, I, and E in both compounds. Our results show that 14–15 halogenido metalates are promising new materials that can expand the useful properties of lead halide perovskites for optoelectronic applications.

Acknowledgements

This work is funded by the by the Deutsche Forschungsgemeinschaft, Project-ID 223848855-SFB 1083 Structure and Dynamics of Internal Interfaces. J.H. thanks Prof. Stefanie Dehnen for her constant support. N.D. thanks the Fonds der Chemischen Industrie and the Studienstiftung des Deutschen Volkes for their support. S.C. acknowledges personal support through the Heisenberg Programme (CH660/08). We thank Michael Hellwig for his help with EDX measurements and RZ Regensburg, GOETHE-CSC, and HLRS Stuttgart for computational resources. Open access funding enabled and organized by Projekt DEAL.

Conflict of interest

The authors declare no conflict of interest.

Keywords: antimony · bismuth · iodine · lead · perovskite

[1] G. Xing, N. Mathews, S. Sun, S. S. Lim, Y. M. Lam, M. Grätzel, S. Mhaisalkar, T. C. Sum, *Science* **2013**, *342*, 344 – 347.
[2] C. C. Stoumpos, M. G. Kanatzidis, *Adv. Mater.* **2016**, *28*, 5778 – 5793.
[3] L. Chouhan, S. Ghimire, C. Subrahmanyam, T. Miyasaka, V. Biju, *Chem. Soc. Rev.* **2020**, *49*, 2869 – 2885.
[4] A. K. Jena, A. Kulkarni, T. Miyasaka, *Chem. Rev.* **2019**, *119*, 3036 – 3103.
[5] Y. Wei, Z. Cheng, J. Lin, *Chem. Soc. Rev.* **2019**, *48*, 310 – 350.
[6] H. Dong, C. Zhang, X. Liu, J. Yao, Y. S. Zhao, *Chem. Soc. Rev.* **2020**, *49*, 951 – 982.
[7] H. Huang, B. Pradhan, J. Hofkens, M. B. J. Roeffaers, J. A. Steele, *ACS Energy Lett.* **2020**, *5*, 1107 – 1123.
[8] D. Ghosh, E. Welch, A. J. Neukirch, A. Zakhidov, S. Tretiak, *J. Phys. Chem. Lett.* **2020**, *11*, 3271 – 3286.
[9] D. B. Straus, C. R. Kagan, *J. Phys. Chem. Lett.* **2018**, *9*, 1434 – 1447.
[10] Q. A. Akkerman, G. Rainò, M. V. Kovalenko, L. Manna, *Nat. Mater.* **2018**, *17*, 394 – 405.
[11] Y. Zhou, J. Chen, O. M. Bakr, H.-T. Sun, *Chem. Mater.* **2018**, *30*, 6589 – 6613.
[12] B. Luo, F. Li, K. Xu, Y. Guo, Y. Liu, Z. Xia, J. Z. Zhang, *J. Mater. Chem. C* **2019**, *7*, 2781 – 2808.
[13] C.-H. Lu, G. V. Biesold-McGee, Y. Liu, Z. Kang, Z. Lin, *Chem. Soc. Rev.* **2020**, *49*, 4953 – 5007.
[14] M. Saliba, T. Matsui, K. Domanski, J. Y. Seo, A. Ummadisingu, S. M. Zakeeruddin, J. P. Correa-Baena, W. R. Tress, A. Abate, A. Hagfeldt, M. Grätzel, *Science* **2016**, *354*, 206 – 209.
[15] E. H. Jung, N. J. Jeon, E. Y. Park, C. S. Moon, T. J. Shin, T.-Y. Yang, J. H. Noh, J. Seo, *Nature* **2019**, *567*, 511 – 515.
[16] C. C. Stoumpos, C. D. Malliakas, M. G. Kanatzidis, *Inorg. Chem.* **2013**, *52*, 9019 – 9038.
[17] Z. Yao, Z. Jin, X. Zhang, Q. Wang, H. Zhang, Z. Xu, L. Ding, S. Liu, *J. Mater. Chem. C* **2019**, *7*, 13736 – 13742.
[18] A. K. Guria, S. K. Dutta, S. D. Adhikari, N. Pradhan, *ACS Energy Lett.* **2017**, *2*, 1014 – 1021.
[19] A. L. Abdelhady, M. I. Saidaminov, B. Murali, V. Adinolfi, O. Voznyy, K. Katsiev, E. Alarousu, R. Comin, I. Dursun, L. Sinatra, E. H. Sargent, O. F. Mohammed, O. M. Bakr, *J. Phys. Chem. Lett.* **2016**, *7*, 295 – 301.
[20] P. K. Nayak, M. Sendner, B. Wenger, Z. Wang, K. Sharma, A. J. Ramadan, R. Lovrinčić, A. Pucci, P. K. Madhu, H. J. Snaith, *J. Am. Chem. Soc.* **2018**, *140*, 574 – 577.
[21] O. A. Lozhkina, A. A. Murashkina, V. V. Shilovskikh, Y. V. Kapitonov, V. K. Ryabchuk, A. V. Emeline, T. Miyasaka, *J. Phys. Chem. Lett.* **2018**, *9*, 5408 – 5411.
[22] A. M. Ulatowski, A. D. Wright, B. Wenger, L. R. V. Buizza, S. G. Motti, H. J. Eggimann, K. J. Savill, J. Borchert, H. J. Snaith, M. B. Johnston, L. M. Herz, *J. Phys. Chem. Lett.* **2020**, *11*, 3681 – 3688.
[23] L. A. Frolova, D. V. Anokhin, K. L. Gerasimov, N. N. Dremova, P. A. Troshin, *J. Phys. Chem. Lett.* **2016**, *7*, 4353 – 4357.
[24] M. Yavari, F. Ebadi, S. Meloni, Z. S. Wang, T. C.-J. Yang, S. Sun, H. Schwartz, Z. Wang, B. Niesen, J. Durantini, P. Rieder, K. Tvingstedt, T. Buonassisi, W. C. H. Choy, A. Filippetti, T. Dittrich, S. Olthof, J.-P. Correa-Baena, W. Tress, *J. Mater. Chem. A* **2019**, *7*, 23838 – 23853.
[25] Y. Hu, T. Qiu, F. Bai, X. Miao, S. Zhang, *J. Mater. Chem. A* **2017**, *5*, 25258 – 25265.
[26] J. Zhang, M.-h. Shang, P. Wang, X. Huang, J. Xu, Z. Hu, Y. Zhu, L. Han, *ACS Energy Lett.* **2016**, *1*, 535 – 541.
[27] S. Xiang, W. Li, Y. Wei, J. Liu, H. Liu, L. Zhu, H. Chen, *Nanoscale* **2018**, *10*, 9996 – 10004.
[28] L. Huang, S. Bu, D. Zhang, R. Peng, Q. Wei, Z. Ge, J. Zhang, *Sol. RRL* **2019**, *3*, 1800274.
[29] H. W. Qiao, S. Yang, Y. Wang, X. Chen, T. Y. Wen, L. J. Tang, Q. Cheng, Y. Hou, H. Zhao, H. G. Yang, *Adv. Mater.* **2019**, *31*, 1804217.
[30] F. Zhu, N. E. Gentry, L. Men, M. A. White, J. Vela, *J. Phys. Chem. C* **2018**, *122*, 14082 – 14090.
[31] Y. Hu, T. Qiu, F. Bai, W. Ruan, S. Zhang, *Adv. Energy Mater.* **2018**, *8*, 1703620.
[32] J. Bartolomé, E. Climent-Pascual, C. Redondo-Obispo, C. Zaldo, Á. L. Álvarez, A. de Andrés, C. Coya, *Chem. Mater.* **2019**, *31*, 3662 – 3671.
[33] E. Mosconi, B. Merabet, D. Meggiolaro, A. Zaoui, F. De Angelis, *J. Phys. Chem. C* **2018**, *122*, 14107 – 14112.
[34] J.-L. Li, J. Yang, T. Wu, S.-H. Wei, *J. Mater. Chem. C* **2019**, *7*, 4230 – 4234.
[35] X. Zhang, J.-X. Shen, M. E. Turiansky, C. G. Van de Walle, *J. Mater. Chem. A* **2020**, *8*, 12964 – 12967.
[36] Y. Zhou, Z.-J. Yong, W. Zhang, J.-P. Ma, A. Sadhanala, Y.-M. Chen, B.-M. Liu, Y. Zhou, B. Song, H.-T. Sun, *J. Mater. Chem. C* **2017**, *5*, 2591 – 2596.
[37] R. Meng, G. Wu, J. Zhou, H. Zhou, H. Fang, M. A. Loi, Y. Zhang, *Chem. Eur. J.* **2019**, *25*, 5480 – 5488.
[38] X. Zhang, H. Wang, Y. Hu, Y. Pei, S. Wang, Z. Shi, V. L. Colvin, S. Wang, Y. Zhang, W. W. Yu, *J. Phys. Chem. Lett.* **2019**, *10*, 1750 – 1756.
[39] W. Tang, J. Zhang, S. Ratnasingham, F. Liscio, K. Chen, T. Liu, K. Wan, E. Suena Galindez, E. Bilotti, M. Reece, M. Baxendale, S. Milita, M. A. McLachlan, L. Su, O. Fenwick, *J. Mater. Chem. A* **2020**, *8*, 13594 – 13599.
[40] K.-z. Du, X. Wang, Q. Han, Y. Yan, D. B. Mitzi, *ACS Energy Lett.* **2017**, *2*, 2486 – 2490.

 © 2020 The Authors. Angewandte Chemie International Edition published by Wiley-VCH GmbH

15213773, 2021, 8, Downloaded from https://onlinelibrary.wiley.com/doi/10.1002/anie.202014696 by Universitaet Regensburg, Wiley Online Library on [18/03/2024]. See the Terms and Conditions (https://onlinelibrary.wiley.com/terms-and-conditions) on Wiley Online Library for rules of use; OA articles are governed by the applicable Creative Commons License

[41] B. Sun, X.-F. Liu, X.-Y. Li, Y. Cao, Z. Yan, L. Fu, N. Tang, Q. Wang, X. Shao, D. Yang, H.-L. Zhang, *Angew. Chem. Int. Ed.* **2020**, *59*, 203 – 208; *Angew. Chem.* **2020**, *132*, 209 – 214.
[42] B. Vargas, E. Ramos, E. Pérez-Gutiérrez, J. C. Alonso, D. Solis-Ibarra, *J. Am. Chem. Soc.* **2017**, *139*, 9116 – 9119.
[43] B. Vargas, R. Torres-Cadena, J. Rodríguez-Hernández, M. Gembicky, H. Xie, J. Jiménez-Mier, Y.-S. Liu, E. Menéndez-Proupin, K. R. Dunbar, N. Lopez, P. Olalde-Velasco, D. Solis-Ibarra, *Chem. Mater.* **2018**, *30*, 5315 – 5321.
[44] B. Vargas, R. Torres-Cadena, D. T. Reyes-Castillo, J. Rodríguez-Hernández, M. Gembicky, E. Menéndez-Proupin, D. Solis-Ibarra, *Chem. Mater.* **2020**, *32*, 424 – 429.
[45] B. Wahl, M. Erbe, A. Gerisch, L. Kloo, M. Ruck, *Z. Anorg. Allg. Chem.* **2009**, *635*, 743 – 752.
[46] B. Wahl, L. Kloo, M. Ruck, *Z. Anorg. Allg. Chem.* **2009**, *635*, 1979 – 1985.
[47] A. Gerisch, M. Ruck, *Z. Kristallogr. - Cryst. Mater.* **2011**, *226*, 613 – 618.
[48] M. F. Groh, A. Wolff, B. Wahl, B. Rasche, P. Gebauer, M. Ruck, *Z. Anorg. Allg. Chem.* **2017**, *643*, 69 – 80.
[49] C. Zhou, S. Lee, H. Lin, J. Neu, M. Chaaban, L.-J. Xu, A. Arcidiacono, Q. He, M. Worku, L. Ledbetter, X. Lin, J. A. Schlueter, T. Siegrist, B. Ma, *ACS Mater. Lett.* **2020**, *2*, 376 – 380.
[50] D. G. Billing, A. Lemmerer, *CrystEngComm* **2006**, *8*, 686 – 695.
[51] G. C. Papavassiliou, I. B. Koutselas, A. Terzis, C. P. Raptopoulou, *Z. Naturforsch. B* **1995**, *50*, 1566 – 1569.
[52] M. Bujak, *Acta Crystallogr. Sect. B* **2017**, *73*, 432 – 442.
[53] M. Lindsjö, A. Fischer, L. Kloo, *Z. Anorg. Allg. Chem.* **2005**, *631*, 1497 – 1501.
[54] T. Baikie, Y. Fang, J. M. Kadro, M. Schreyer, F. Wei, S. G. Mhaisalkar, M. Grätzel, T. J. White, *J. Mater. Chem. A* **2013**, *1*, 5628 – 5641.
[55] V. Yu. Kotov, A. B. Ilyukhin, P. A. Buikin, K. E. Yorov, *Mendeleev Commun.* **2019**, *29*, 537 – 540.
[56] Y. Morgenstern, F. Zischka, A. Kornath, *Chem. Eur. J.* **2018**, *24*, 17311 – 17317.
[57] M. J. Molski, M. A. Khanfar, H. Shorafa, K. Seppelt, *Eur. J. Org. Chem.* **2013**, 3131 – 3136.
[58] D. B. Mitzi, *Chem. Mater.* **1996**, *8*, 791 – 800.
[59] G.-E. Wang, X.-M. Jiang, M.-J. Zhang, H.-F. Chen, B.-W. Liu, M.-S. Wang, G.-C. Guo, *CrystEngComm* **2013**, *15*, 10399 – 10404.
[60] N. Dehnhardt, P. Klement, S. Chatterjee, J. Heine, *Inorg. Chem.* **2019**, *58*, 10983 – 10990.
[61] Y. Yamada, M. Hoyano, R. Akashi, K. Oto, Y. Kanemitsu, *J. Phys. Chem. Lett.* **2017**, *8*, 5798 – 5803.
[62] S. Li, J. Luo, J. Liu, J. Tang, *J. Phys. Chem. Lett.* **2019**, *10*, 1999 – 2007.
[63] K. M. McCall, C. C. Stoumpos, S. S. Kostina, M. G. Kanatzidis, B. W. Wessels, *Chem. Mater.* **2017**, *29*, 4129 – 4145.
[64] J. P. Perdew, K. Burke, M. Ernzerhof, *Phys. Rev. Lett.* **1996**, *77*, 3865 – 3868.
[65] S. Grimme, J. Antony, S. Ehrlich, H. Krieg, *J. Chem. Phys.* **2010**, *132*, 154104.
[66] S. Grimme, S. Ehrlich, L. Goerigk, *J. Comput. Chem.* **2011**, *32*, 1456 – 1465.
[67] F. Tran, P. Blaha, *Phys. Rev. Lett.* **2009**, *102*, 226401.
[68] N. Dehnhardt, J.-N. Luy, M. Szabo, M. Wende, R. Tonner, J. Heine, *Chem. Commun.* **2019**, *55*, 14725 – 14728.
[69] Sandeep, D. P. Rai, A. Shankar, M. P. Ghimire, R. Khenata, S. Bin Omran, S. V. Syrotyuk, R. K. Thapa, *Mater. Chem. Phys.* **2017**, *192*, 282 – 290.
[70] Z. Xiao, W. Meng, J. Wang, D. B. Mitzi, Y. Yan, *Mater. Horiz.* **2017**, *4*, 206 – 216.
[71] Deposition Numbers 2038624 – 2038625 contain the supplementary crystallographic data for this paper. These data are provided free of charge by the joint Cambridge Crystallographic Data Centre and Fachinformationszentrum Karlsruhe Access Structures service www.ccdc.cam.ac.uk/structures.

Manuscript received: November 3, 2020
Accepted manuscript online: November 30, 2020
Version of record online: January 15, 2021

 © 2020 The Authors. Angewandte Chemie International Edition published by Wiley-VCH GmbH

15213773, 2021, 8, Downloaded from https://onlinelibrary.wiley.com/doi/10.1002/anie.202014696 by Universitaet Regensburg, Wiley Online Library on [18/03/2024]. See the Terms and Conditions (https://onlinelibrary.wiley.com/terms-and-conditions) on Wiley Online Library for rules of use; OA articles are governed by the applicable Creative Commons License